ISSN 1330-3651 (Print), ISSN 1848-6339 (Online)
https://doi.org/10.17559/TV-20250117002277
Original scientific paper

Orientation Recognition of Shallow Buried Target in Homogeneous Medium

Yanlong ZHU*, Xiangshang SU

Abstract: According to the characteristics of energy equality and pole convergence under different polarization conditions, the start of the transient late-time response of shallow buried target can be accurately estimated. By quantitatively comparing the late-time response of theta polarization and phi polarization at different incident angles, the quantitative relationship among incident angle, target orientation information and late-time response statistics is obtained. Basing on the variance of the late-time response under two polarizations at different incident angles, the orientation recognition of slender target in homogeneous medium is realized.

Keywords: homogeneous medium; orientation recognition; polarimetric ground penetrating radar; shallow buried target

1 INTRODUCTION

Ground penetrating radar (GPR), as a fast, continuous, non-contact electromagnetic wave surface detection method [1], is widely used in engineering detection [2], environmental protection, cultural relics archaeology [3], resource exploration and many other scientific discipline fields [4].

GPR is based on the reflection principle of advanced transient electromagnetic pulse [5]. The Gaussian pulse signal with extremely narrow time-domain width is used as the incident signal to irradiate the buried target. During the propagation of electromagnetic waves underground, when encountering target with different electrical properties, the reflection and refraction will occur. The target reflection and backscattering signal received by the receiving antenna is the time-domain transient response of the target. In the Singularity Expansion Method (SEM) theory, the time domain transient response of the target consists of two parts: the early-time response and the late-time response [6]. The early-time response includes the optical scattering signal of different scattering centers and the modulated signal generated by the target body, which reflects the position information of the target scattering center. The late-time response includes the radiated signal generated by the induced current, which reflects the natural characteristics of the target [7], such as the natural complex resonance frequency, namely the pole characteristic information. Because the distribution law of poles is only related to the external shape of the target, and is independent of the incident wave, polarization mode and the attitude of the target [8], it is mostly used in the field of target recognition.

The pole information contained in the late-time response can be used to identify shallow buried target, provided that the start of the late-time response must be accurately judged. In reference [9], a set of poles corresponding to the late-time response in each time window is estimated by setting multiple continuous time windows, and the boundary between the early-time response and late-time response of the cylinder in free space is deuced by using the convergence of poles. With the maturing of polarization technology, polarization GPR has been applied in various engineering and technical fields. In reference [10], the polarization electromagnetic wave generated by GPR enhances the deep detection ability for highway bridges which avoid the strong interference of the shallow steel bars. In reference [11], the early-time response can be suppressed by using polarization differences, but the polarization characteristics between the early-time response and late-time response must be significantly different. In reference [12], the expression of electric field intensity at far field under each polarization by using two mutually orthogonal polarization states is derived, and the early-time response and the late-time response are successfully separated through theoretical analysis. In reference [13], on the premise of equal energy of surface reflected wave in the early-time response, determine the beginning point of windowing processing, sample the time window of the time domain transient response data after the beginning point, construct Hankel matrix according to the windowed data, calculate the singular value of each matrix, the time when the maximum singular value suddenly decreases is the start of late-time response. In reference [14], according to the pole convergence contained in the late-time response, set a reasonable time window and step size and estimate the pole by the Matrix Pencil Method (MPM); the earliest convergence time is the start of the late-time response. This processing method can accurately separate the late-time response and effectively determine the location of the target, which is helpful to make full use of the information contained in the early-time and late-time response. Reference [15] proposed a polarimetric ground penetrating radar system based on gray complementary code. The gray complementary code is used as the detection signal to obtain the polarization data of the underground pipeline echo by changing the polarization mode of the antenna, so as to realize the pipeline distribution detection. Reference [16] used full polarization ground penetrating radar to derive the relationship between different parameters and measurement angle and infiltration time, so as to judge the severity of fluid fractures, and broaden the application scenarios of polarization ground penetrating radar.

In this paper, the estimation algorithm of the start of late-time response of shallow buried slender target in homogeneous medium is used to isolate the transient late-time response at any incident angle. The transient late-time response of theta and phi under a group of orthogonal polarization at multiple incident angles is analyzed in detail to determine the relationship among incident angles, target orientation information and late-time response statistics.

The variance of late-time response under orthogonal polarization at different incident angles is compared to realize the orientation recognition of slender target in homogeneous medium.

2 THEORETICAL ANALYSIS OF TARGET ORIENTATION RECOGNITION

2.1 The GPR Detection Model

The GPR detection model is shown in Fig. 1. There is a slender cylindrical target in homogeneous medium, and the axial direction of the cylinder is arbitrary. The transmitting end uses a Gaussian pulse signal source to irradiate the target in the form of a certain incident angle, and the receiving end uses an antenna to receive the backscattered signal data of the target. By changing the irradiation angle and polarization mode of the incident wave, the backscattered signals of the target at different incident angles and polarization are obtained, and the template information database of the multi-directional transient response of the target is established. When the incident wave irradiates the target at a certain angle, the orientation information of the target can be determined by comparing the feature information processed by the algorithm with the relationship in the template information database.

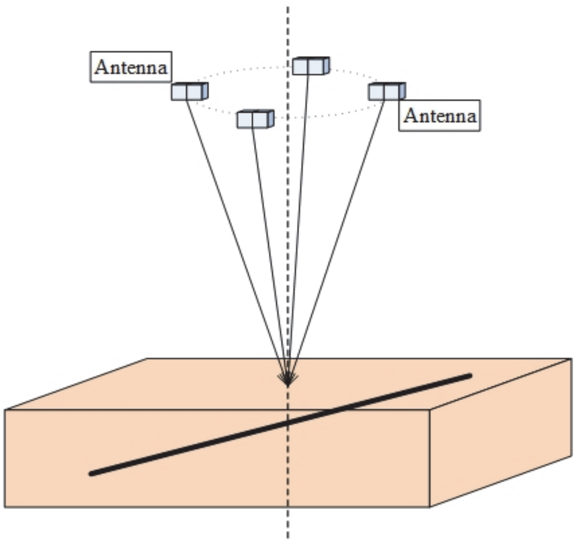

Figure 1 The GPR Detection Model

2.2 Algorithm theory

Any substance that has an electrical effect is called a dielectric. A certain amount of charge is bound in the dielectric. According to the distribution characteristics, the molecules of the dielectric are divided into non-polar molecules and polar molecules. The positive and negative charge centers of non-polar molecules coincide, so the resultant electric field generated externally is zero, and does not show electrical characteristics. The positive and negative charge centers of polar molecules are not in the same position and form electric dipoles with each other. Such electric dipoles are distributed inside the dielectric and arranged randomly, resulting in the total electric dipole moments canceling each other. Therefore, the resultant electric field generated externally is also zero. Under the action of an external electric field, the bound charge in the dielectric shifts, and it is called dielectric polarization. The polarization of the dielectric makes countless electric dipoles in the dielectric arranged along the direction of the external electric field, thus changing the original electric field distribution. When the external electric field disappears, the additional electric field generated by the polarized charge makes the dielectric produce induced current, and the backscattered signal received after outward radiation is the transient late-time response of the target.

Polarization intensity is the vector sum of dipole moments per unit volume, which can measure the polarization degree of different dielectrics. The expression is:

$$\vec{P} = \lim_{\Delta V \to 0} \frac{\sum_i \vec{p}_i}{\Delta V} \tag{1}$$

where $p_i = q_i d_i$ is the average electric dipole moment of the *i* in volume ΔV , P is a macroscopic vector function. If the P of each point within a certain area of the dielectric is the same, the area is considered to be uniformly polarized, otherwise, it is non-uniform polarized. Obviously, the greater the polarization intensity, the greater the electric field intensity that generates the external electric field.

In the GPR detection model, assume the length, width and height of the medium are a, b, c the length of slender cylinder in medium is l , the radius is r . When the incident plane wave is perpendicular to the target, the average electric dipole moment under theta polarization is:

$$\sum \vec{p}_{\theta,cub} + \sum \vec{p}_{\theta,cyl} = bc \cdot a \cdot \vec{e}_\theta p_{\theta,cub} + \pi r^2 \cdot h \cdot \vec{e}_\theta p_{\theta,cyl} \tag{2}$$

where $p_{\theta,cub}$ and $p_{\theta,cyl}$ are the average electric dipole moments of dielectric cuboid and target cylinder under theta polarization respectively.

The average electric dipole moment under phi polarization is:

$$\sum \vec{p}_{\varphi,cub} + \sum \vec{p}_{\varphi,cyl} = ac \cdot b \cdot \vec{e}_\varphi p_{\varphi,cub} + \Delta rh \cdot 2r\vec{e}_\varphi p_{\varphi,cyl} \tag{3}$$

where $p_{\varphi,cub}$ and $p_{\varphi,cyl}$ are the average electric dipole moments of dielectric cuboid and target cylinder under phi polarization respectively. Since the axial length of the cylinder with conductor properties is far greater than the radius of the cross section, it can be considered as a long, straight and thin wire. Therefore, when $\Delta r \to 0$, $\sum \vec{p}_{\varphi,cyl} \to 0$, it means that the polarization intensity of the slender cylinder caused by the applied electric field is very small and can be ignored under phi polarization.

Thus, the polarization intensity caused by theta and phi polarization can be calculated as follows:

$$\begin{aligned} \vec{P}_\theta &= \left(\sum \vec{p}_{\theta,cub} + \sum \vec{p}_{\theta,cyl}\right) / V = \\ &= \vec{e}_\theta p_{\theta,cub} + \left(\pi r^2 \cdot h / V\right) \vec{e}_\theta p_{\theta,cyl} \end{aligned} \tag{4}$$

$$\vec{P}_\varphi = \left(\sum \vec{p}_{\varphi,cub} + \sum \vec{p}_{\varphi,cyl}\right) \Big/ V = \\ = \vec{e}_\varphi p_{\varphi,cub} \tag{5}$$

where, $p_{\theta,cub} = p_{\varphi,cub}$ .The internal charge activity of the conductive object is more intense than that of the dielectric body, so the electric dipole moment generated is larger. According to Eq. (4) and Eq. (5), when the incident wave is perpendicular to the target, the average polarization intensity of the target under theta is much greater than that under phi polarization, so the corresponding electric field intensity under the two polarizations is:

$$\left|\vec{E}_{Late,\perp\theta}\right| > \left|\vec{E}_{Late,\perp\varphi}\right| \tag{6}$$

In general, the transient late-time response of the target is the signal radiated outward by the induced current generated by the target, which is the linear superposition of a series of damping oscillation curves. The mean value of late-time response can be expressed as:

$$\mu = \lim_{T\to\infty} \frac{1}{T}\int_0^T e^{\sigma + j\omega} d\omega = 0 \tag{7}$$

Obviously, the mean value under theta polarization and phi polarization is zero. The variance under two polarizations is:

$$D_{\perp\theta} = E\left[\left(E_{Late,\theta} - E\left(E_{Late,\theta}\right)\right)^2\right] \tag{8}$$

$$D_{\perp\varphi} = E\left[\left(E_{Late,\varphi} - E\left(E_{Late,\varphi}\right)\right)^2\right] \tag{9}$$

Comparing the above four Eq. (6), Eq. (7), Eq. (8) and Eq. (9), the result can be obtained:

$$D_{\perp\theta} > D_{\perp\varphi} \tag{10}$$

When the incident wave is perpendicular to the target, the variance under theta polarization is greater than that under phi polarization. In other words, the deviation of the electric field intensity value from the mean value under theta polarization is greater than that under phi polarization, which also indicates that the electric field intensity under theta polarization is greater than that under phi polarization.

When the incident wave irradiates the target at a certain angle, the direction of the electric field intensity in the electromagnetic wave is not always parallel to the axial direction of the target. According to the parallelogram vector algorithm, the electric field can always be decomposed into axial components. Since the intensity of the incident wave is the same, the decomposed components are relatively small. Therefore, when the incident wave slants the target, the electric field intensity of the late-time response generated under theta polarization is always less than or equal to $\left|\vec{E}_{Late,\perp\theta}\right|$, the electric field intensity of the late-time response generated under phi polarization is always greater than or equal to $\left|\vec{E}_{Late,\perp\varphi}\right|$. The variance of late-time response under different polarizations is the same. When the incident wave is perpendicular to the target, theta polarization and phi polarization have the maximum and minimum electric field intensity values respectively, and the difference between them is the largest in all incident angles.

To sum up, the transient late-time response under different polarization conditions at different incident angles on the surface half space approximately follows the standard normal distribution with a mean of zero, and has a set of constant variance values D_θ and D_φ. The data of different groups are independent of each other. Under the premise of significance level of 0.05, F value test was used:

$$H_0 : D_\theta / D_\varphi = 1 \tag{11}$$

$$H_1 : D_\theta / D_\varphi \neq 1 \tag{12}$$

where H_0 and H_1 represent two assumptions for the comparison of the difference between the two polarizations. If hypothesis H_0 is accepted, it represents that the variances under two polarizations are equal, indicating homogeneity of variances. Otherwise, if hypothesis H_1 is accepted, it represents that the variances under the two polarizations are not equal, indicating heteroscedasticity. Therefore, through F value test, according to the incident angle corresponding to the value with the largest variance difference, the orientation information of slender target can be realized.

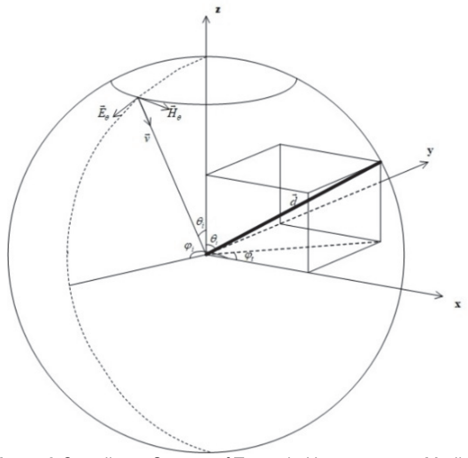

Figure 2 Coordinate System of Target in Homogeneous Medium

As shown in Fig. 2, it is the coordinate system of target in homogeneous medium. The direction of the slender target is $\vec{d}$, the azimuth angle is φ_t , the pitch angle is θ_t . Assuming the direction of the incident plane wave is $\vec{v}$, the corresponding azimuth and pitch angles are φ_i and θ_i , taking theta polarization mode as an example, the electric field intensity direction, magnetic field intensity direction and wave speed propagation direction conform to the right hand rectangular coordinate system, where the electric field intensity direction follows the direction of theta change in the coordinate system. According to the parallelogram rule, the electric field of the plane wave at any incident angle produces components in direction $\vec{d}$, if and only if the direction of the electric field intensity is parallel to the direction of the slender target, the electric field intensity of the late-time response is the largest, i.e:

$$\vec{d}\times\vec{v}_\theta=0 \tag{13}$$

From the relationship between spherical coordinate system and space rectangular coordinate system, it can be seen that:

$$\vec{d}=\vec{e}_x\sin\theta_t\cos\varphi_t+\vec{e}_y\sin\theta_t\sin\varphi_t+\vec{e}_z\cos\theta_t \tag{14}$$

$$\vec{v}_\theta=\vec{e}_x\cos\theta_i\cos\varphi_i+\vec{e}_y\cos\theta_i\sin\varphi_i-\vec{e}_z\sin\theta_i \tag{15}$$

Substituting Eq. (14) and Eq. (15) into Eq. (13):

$$\vec{d}\times\vec{v}_\theta=\begin{vmatrix}\vec{e}_x & \vec{e}_y & \vec{e}_z\\ \sin\theta_t\cos\varphi_t & \sin\theta_t\sin\varphi_t & \cos\theta_t\\ \cos\theta_i\cos\varphi_i & \cos\theta_i\sin\varphi_i & -\sin\theta_i\end{vmatrix}=0 \tag{16}$$

Simplify Eq. (16):

$$\begin{cases}\sin\theta_t\sin\varphi_t\sin\theta_i+\cos\theta_i\sin\varphi_i\cos\theta_t=0\\ \sin\theta_t\cos\varphi_t\sin\theta_i+\cos\theta_i\cos\varphi_i\cos\theta_t=0\\ \sin\theta_t\cos\varphi_t\cos\theta_i\sin\varphi_i-\cos\theta_i\cos\varphi_i\sin\theta_t\sin\varphi_t=0\end{cases} \tag{17}$$

Solve the equation set Eq. (17):

$$\begin{cases}\varphi_i-\varphi_t=k\cdot\pi, k=0,\pm1,\pm2\cdots\\ \theta_i+\theta_t=k\cdot\dfrac{\pi}{2}, k=\pm1,\pm3,\pm5,\cdots\end{cases} \tag{18}$$

Generally, in the application of detecting underground pipelines, cracks and water filling characteristics, GPR only work in the half space of the surface, therefore:

$$0\le\varphi_i,\varphi_t<2\pi \tag{19}$$

$$0\le\theta_i,\theta_t\le\frac{\pi}{2} \tag{20}$$

By comparing Eq. (18), Eq. (19) and Eq. (20), it can be seen that:

$$\varphi_i-\varphi_t=\pi \tag{21}$$

$$\theta_i+\theta_t=\frac{\pi}{2} \tag{22}$$

In general, the direction of incident plane waves is determined according to the late-time response information at different incident angles, and the orientation information of the slender target can be realized by using Eq. (21) and Eq. (22).

3 SIMULATION RESULTS AND ANALYSIS

The steps of orientation recognition of slender cylindrical target in homogeneous medium are:
(1) Obtain the discrete sampling data at different incident wave angles;
(2) According to the pole convergence characteristics, the discrete data are processed by using the estimation algorithm of the start of late-time response of slender target in homogeneous medium, and the late-time response under theta and phi polarization at different incident angles are obtained;
(3) Calculate the mean and variance of the late-time response at different incident angles;
(4) By comparing the variance of the two polarizations at different angles, the parameters of the incident plane waves are derived, so as to determine the orientation information of the slender target.

XFDTD software is an electromagnetic simulation tool based on finite difference time domain fumla method, which is mainly used for modeling and calculation of high-frequency electromagnetic problems. The simulation model in XFDTD software is shown in Fig.3. Suppose that the target is a slender cylinder with high conductivity, the axial direction of the slender cylinder is parallel to the Y axis, the azimuth angle is $\varphi=90^\circ$, the pitch angle is $\theta=90^\circ$, the buried depth h is 50 mm, the axial length l is 700 mm, and the radius of the cross-section circle a is 5 mm. The incident wave is an ultra wideband pulse source with a half width of 1ns. The homogeneous medium is dry sand, the relative dielectric constant is 4, the conductivity is 0.001 s/m, and the length is 800 mm, the width is 800 mm and the height is 400 mm.

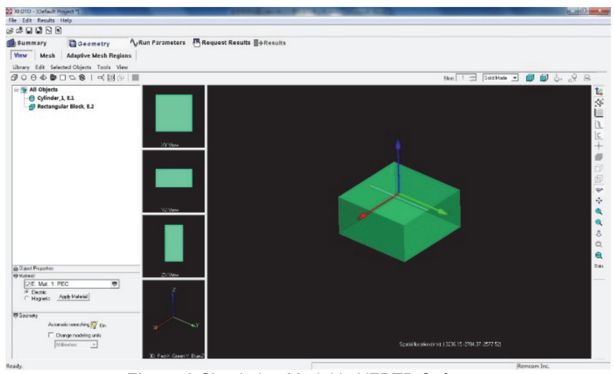

Figure 3 Simulation Model in XFDTD Software

In the spherical coordinate system, the direction of the incident plane wave can be determined by setting the values of the parameters φ and θ. The azimuth angle φ are taken a group data every 30° within the rangle of $0^\circ\sim330^\circ$, the pitch angle θ are taken as 0°, 5°, 10°, 30°, 45°, 60°, 75°, 90°. At the same incident angle, theta and phi polarization are used to irradiate the target. A total of 192 groups of time-domain transient response data are obtained, including 96 groups of theta polarization data and 96 groups of phi polarization data.

According to the pole convergence characteristic contained in the late-time response, the late-time response at each incident angle is separated. Taking the incident angle $\varphi = 270^\circ$ as an example, the distribution of the start of late-time response at each pitch angle is obtained in Fig. 4. The black dotted line marks the start of late-time response at different pitch angles. At the beginning, the electric field intensity direction of the incident plane wave is parallel to the target. As the pitch angle increases, the incident plane wave generates components along the axial direction of the slender target and gradually decreases until the electric field intensity direction is perpendicular to the axial direction of the target. In the whole process, the start of late-time response gradually lags behind.

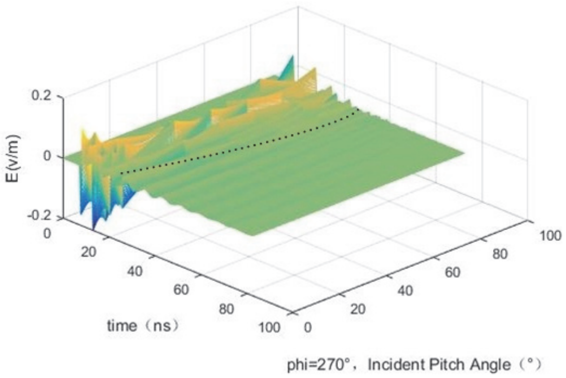

Figure 4 The Start of Late-time response at Different Pitch Angles, when phi=270°

The statistical analysis diagram of the mean value of late-time response under theta and phi polarization is shown in Fig. 5 and Fig. 6. It can be seen that the mean value of late-time response under the two polarizations fluctuates around zero and approaches zero. Theoretically, the mean value of late-time response of the target is zero. Therefore, within the allowable error range, the simulation data is almost consistent with the theory. The error mainly comes from two aspects: firstly, the simulation software itself is an approximate numerical calculation of electromagnetic wave, which has certain error; secondly, the data processed in this paper truncates the part of the original data approaching zero at the end, which has a certain impact on the calculation result. The mean error under both polarizations is less than one thousandth.

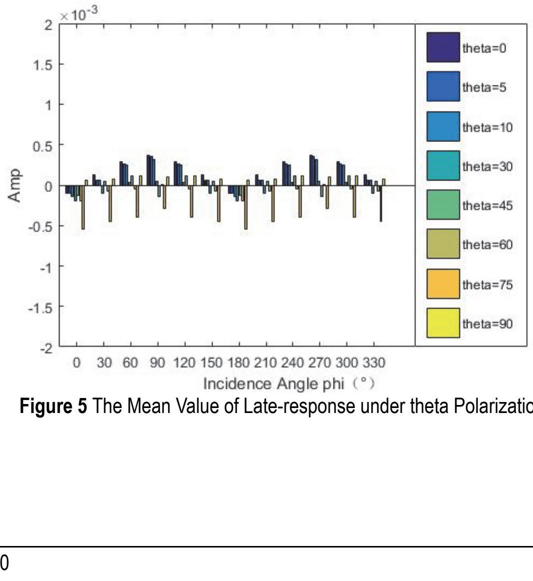

Figure 5 The Mean Value of Late-response under theta Polarization

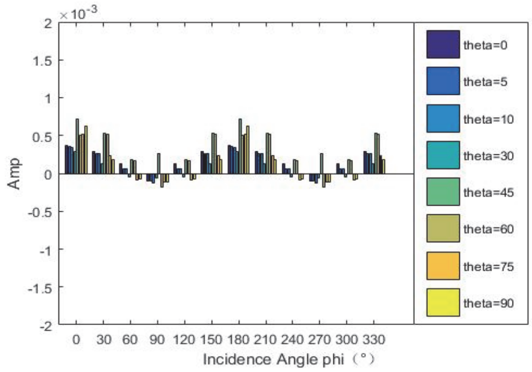

Figure 6 The Mean Value of Late-response under phi Polarization

The mean value of late-time response at different incident plane wave angles basically approaches zero, and the difference is very small. Considering that the late-time response of the target is approximately subject to the standard normal distribution, it can be regarded as samples from different populations, and the samples are independent of each other. Due to the difference of polarization intensity, the variance of late-time response varies greatly at different incident angles. Taking the incident angle $\varphi = 270^\circ$ as an example, Fig. 7 shows the variance ratio of theta polarization and phi polarization at different theta angles.

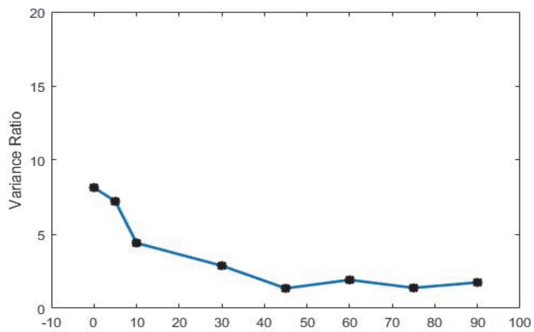

Figure 7 The Variance ratio at Different Theta Angles, when phi=270

As the pitch angle θ increases, the variance ratio of theta and phi polarization gradually decreases. When the target is vertically irradiated by an incident plane wave, the polarization intensity is the largest under theta polarization, resulting in large amplitude of the late-time response, which makes the range of discrete values larger. From the perspective of probability distribution theory, for the standard normal distribution with the mean value of zero, the more scattered the range of discrete values, the greater the degree of deviation from the mean value, and the greater the variance. The direction of electric field intensity is perpendicular to the target under phi polarization, and the D_θ / D_φ is the largest at this time. When the pitch angle changes gradually, the direction of the electric field intensity under theta polarization also changes, the component of the electric field in the axial direction of the target body becomes smaller and smaller, the polarization intensity becomes smaller, and the variance also decreases gradually. The electric field under Phi polarization does not change with the change of pitch angle, and the direction is always perpendicular to the target and remains unchanged. Therefore, the ratio D_θ / D_φ is gradually decreasing.

Table 1 The F Value of Different Incident Angles

F	$\theta = 0^{\circ}$	$\theta = 5^{\circ}$	$\theta = 10^{\circ}$	$\theta = 30^{\circ}$	$\theta = 45^{\circ}$	$\theta = 60^{\circ}$	$\theta = 75^{\circ}$	$\theta = 90^{\circ}$
$\varphi = 0^{\circ}$	0.1092	0.1653	0.1627	0.1127	0.2744	0.3551	0.4711	0.1797
$\varphi = 30^{\circ}$	0.3119	0.2405	0.2346	0.1680	0.1898	0.4020	0.7532	0.5435
$\varphi = 60^{\circ}$	3.0084	3.9320	2.7492	1.6024	1.3306	1.3812	1.4540	1.5407
$\varphi = 90^{\circ}$	8.0793	7.0206	4.0066	2.5614	1.0491	1.5389	1.3969	1.6395
$\varphi = 120^{\circ}$	3.4084	3.7320	2.5492	1.7024	1.3406	1.3912	1.6540	1.7407
$\varphi = 150^{\circ}$	0.3219	0.2305	0.2246	0.1580	0.1798	0.4420	0.7832	0.5335
$\varphi = 180^{\circ}$	0.1193	0.1153	0.1227	0.1327	0.2944	0.3751	0.4911	0.1998
$\varphi = 210^{\circ}$	0.3419	0.2205	0.2446	0.1780	0.2098	0.4220	0.7732	0.5135
$\varphi = 240^{\circ}$	3.1084	3.6320	2.6492	1.9024	1.3406	1.3611	1.7401	1.8407
$\varphi = 270^{\circ}$	8.1452	7.2138	4.4052	2.8715	1.3451	1.9167	1.3757	1.7435
$\varphi = 300^{\circ}$	3.2084	3.8320	2.8492	1.8024	1.3506	1.3511	1.5401	1.9407
$\varphi = 330^{\circ}$	0.3319	0.2105	0.2146	0.1480	0.1898	0.4320	0.7932	0.5235

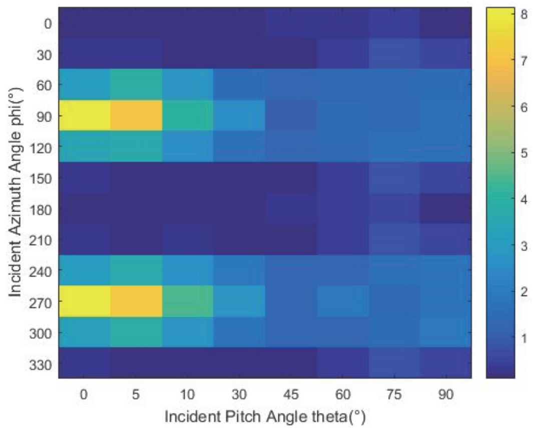

Figure 8 The *F* Value of Different Incident Angles in MATLAB Software

At other incident angles, the direction of the electric field intensity under theta polarization is always at a certain angle with the slender target, and the variance value is smaller than that in the vertical case. The electric field intensity under phi polarization will produce a component in the axial direction of the target, making the variance value larger than that in the vertical case. For the late-time response at all incident angles of plane waves, calculate their respective variance values, and test the variance difference between theta and phi polarization at the same angle by *F* value, The *F* value represents the degree of difference between the two samples. The greater its value, the greater the difference of variance value between the two polarizations. At this time, the incidence angle is perpendicular to the axis of the slender target. The distribution table of F value at each incident angle is shown in Table 1, and the corresponding amplitude gray image in MATLAB software is shown in Fig. 8. Obviously, $\varphi = 270^{\circ}$, $\theta = 0^{\circ}$ in the table 1 is the incident angle with the maximum *F* value, the intensity of the corresponding gray image is also the strongest. According to Eq. (21) and Eq. (22), it can be determined that the direction angle information of the target is $\varphi = 90^{\circ}$, $\theta = 90^{\circ}$, and the orientation recognition of the slender target is realized.

4 CONCLUSION

In this paper, an orientation recognition algorithm of shallow buried slender cylindrical target in homogeneous medium is proposed, which can be applied to the detection of subgrade structure, the identification of underground pipelines, the exploration of mineral resources and other fields. The phenomenon of dielectric polarization is explained from the micro perspective of electromagnetic field, the theoretical derivation is the foundation of target orientation recognition. Using the estimating algorithm for the start of late-time response of shallow buried slender cylindrical target in homogeneous medium and extending it to the case of any incidence angle in the surface half space, the late-time response at any incidence angle is successfully separated. The late-time response under theta and phi polarizations at different incident angles is quantitatively analyzed, and the relationship among the incident angle, target orientation information and late-time response statistics is obtained. Based on the variance of the late-time response at different incident angles under the two polarizations, the orientation recognition of slender target in homogeneous medium is realized. The XFDTD numerical simulation results show that the algorithm can accurately predict the orientation information of shallow buried slender target. For the problem of target orientation recognition in inhomogeneous medium, a region-partitioning approach can be adopted to enhance the adaptability of the proposed algorithm.

5 REFERENCES

[1] Xu, T., Geng, D. X., Cao, J. W., et al. (2025). GPR image recognition for roadbeds disaster based on texture features and support vetor machines. *Chinese Journal of Engineering Geophysics*, *22*(01), 65-73.

[2] Liu, H., Zhang, B., Ding, F., et al. (2024). Enhanced imaging of reinforcement by dual-polarization ground penetrating radar. *Progress in Geophysics*, 1-12.

[3] Meng, T. H., Huang, L., Zhang, H. J., et al. (2024). Application of high-frequency ground penetrating radar in the evaluation of ancient city wall restoration effect. *Geotechnical Engineering Technique*, *38*(02), 196-202.

[4] Zhu, X. M., Fu, M. L., Lu, H. P., et al. (2025). Acquiring the soil stratification of soda saline-alkali soils using ground penetrating radar. *Transactions of the Chinese Society of Agricultural Engineering*, *41*(04), 99-107.

[5] Du, X. B., Zhang, X., & Ding, W. Q. (2024). Automatic classification of ground penetrating radar images based on unsupervised learning. *Chinese Journal of Engineering*

Geophysics, *21*(06), 1068-1077.

[6] Baum, C.E. (1976). *The singularity expansion method*. Springer-Verlag. https://doi.org/10.1007/3540075534_8

[7] Hutchinson, S., Fernando, M., Andrews, D., et al. (2013). Investigation of Late Time Response analysis for detection of multiple concealed objects. In *Electro-Optical Remote Sensing, Photonic Technologies, and Applications VII; and Military Applications in Hyperspectral Imaging and High Spatial Resolution Sensing*, 8897, 225-237. SPIE. https://doi.org/10.1117/12.2028378

[8] Guan, X. P., Wang, S. G, Su, Y., et al. (2004). Analysis of the invariability of target electromagnetic scattering poles. *Journal of Microwaves*, (2), 1-5.

[9] Hong, S. K., Wall, W. S., Andreadis, T. D., et al. (2012). Practical implications of pole series convergence and the early-time in transient backscatter. Naval Research Laboratory. https://doi.org/10.21236/ADA559950

[10] Guo, S. L., Cai, J. C., Zhang, X. Q., et al. (2012). Research on bridges hidden diseases detection method by GPR. *Progress in Geophysics*, *27*(4).

[11] Baum, C.E. (2013). Polarimetric suppression of early-time scattering for late-time target identification. *Ultra-wide-band and Ultra-short Impulse Signals*, 2010, 12-15. https://doi.org/10.1109/UWBUSIS.2010.5609080

[12] Zhou, L. J., Ou-Yang, S., & Jin, L. N. (2013). Extracting turn-on time for analyzing transient scattered response of wire structures. In *Signal and Information Processing* , 49-53. https://doi.org/10.1109/ChinaSIP.2013.6625295

[13] Zhu, Y. L., Liu, C., & Li, Z. H. (2021). Research on treatment of transient response for buried target in large forest. *Forest Chemical Review*, 53-63.

[14] Zhu, Y. L., Zhou, L. J., & Ou-Yang, S. (2016). An estimating method for the start of the transient late-time response of ground penetrating radar. *Journal of Signal Processing*, *32*(1), 98-104.

[15] Zhang, N., Li, J. X., Xu, H, et al. (2022). Underground pipeline distribution detection by polarized ground penetrating radar based on gray complementary code. *Chinese Journal of Electron Devices*, *45*(04), 767-774.

[16] Dong, Z. Q., Feng, X., & Zhou, H. Q. (2023). A study on the characteristics of full-polarimetric ground penetrating radar signals from fractures with fluid flow under different measurement angles. *Modern Radar, 45*(12), 15-23.

Contact information:

Yanlong ZHU
(Corresponding author)
Zhengzhou Railway Vocational & Technical College,
Zhengzhou, Henan, China
E-mail: zhuyanlong_zrvtc@163.com

Xiangshang SU
Zhengzhou Railway Vocational & Technical College
Zhengzhou, Henan, China